Thermal Properties of Epoxidized Natural Rubber-Based Polymer Blends

C. H. Chan, S. F. Sulaiman, H. W. Kammer, L. H. Sim, M. K. Harun

Faculty of Applied Sciences, Department of Chemistry, Universiti Teknologi MARA, 40450 Shah Alam, Malaysia

Received 22 March 2010; accepted 5 September 2010
DOI 10.1002/app.33384
Published online 1 December 2010 in Wiley Online Library (wileyonlinelibrary.com).

ABSTRACT: Thermal properties and morphologies of different thermoplastic polymers blended with an elastomer are discussed. Poly(ethylene terephthalate) (PET), poly(3-hydroxybutyrate-*co*-3-hydroxyvalerate) with 12%mole of hydroxyvalerate content (PHBV) and poly(ethylene oxide) (PEO) were blended with epoxidized natural rubber (ENR). These blends turn out to be immiscible. Degree of crystallinity after isothermal crystallization and equilibrium melting point of the crystallizable constituents stay constant to a good approximation in blends with ENR. Exponential decay of rate of crystallization could be observed for both neat polymers and blends. Morphology formation was observed under condition of constant rate of crystallization, which is concomitantly related to different distances to equilibrium. It turns out that morphology development in the blends reflects both aspects. © 2010 Wiley Periodicals, Inc. J Appl Polym Sci 120: 1774–1781, 2011

Key words: epoxidized natural rubber; thermoplastic; thermal properties; morphologies

INTRODUCTION

Blending of polymers is a useful technique. Extended research activities led it to a well-established technology because blending allows for finely tuning of properties by compositional change. It turns out to be an alternative approach for generating new materials as compared with direct synthesis of polymer systems with desired properties. Blends of elastomers and thermoplastics have been studied extensively.[1–5] Knowledge on thermal properties of those systems is important for efficient adjustment of structure-property relationships. These relationships are governed to a large extent by the phase morphology developing in the blend and formation of supermolecular crystalline structures. Phase morphology is controlled by molecular interactions between the constituents and mixing conditions, whereas the latter by external conditions of crystallization.[6–9] The blends studied in this article contain an amorphous and a semicrystalline polymer, which are completely immiscible in the melt, that is the phases contain only the respective pure polymers. Formation of morphologies under conditions of this study is chiefly ruled by blend composition and thermal history. In all cases, the blends form either dispersions or cocontinuous morphologies, depending on composition. Amorphous and semicrystalline phases coexist in the blends. A narrow interfacial region might develop between the two phases controlling adhesion between them. As a result, one expects intensive quantities, characterizing the blend, to be independent of blend composition. On the other hand, morphology formation is strongly coined by thermal history.[10] Therefore, it is necessary to study crystallization and melting behavior of a constituent in a heterogeneous blend. This serves also to elucidate interfacial interaction and may facilitate search for efficient compatibilizing agents.

Epoxidized natural rubber (ENR) is chemically modified natural rubber (NR). The modification involves the replacement of the double bond in the isoprene units by epoxide groups.[11] ENR with different mol % epoxidation has been shown to be polar and with properties similar to those of acrylonitrile butadiene rubber and butyl rubber. ENR exhibits enhanced oil resistance and decreased gas permeability, while retaining many of the properties of NR with additional interesting properties.[12] The presence of oxirane group in ENR is found to be effective in causing specific interaction with a second polymer.[13–16] This also includes melt reactions at sufficiently high temperatures.[5,17–19]

In this study, ENR with 50 mol % of epoxy content is blended with different crystallizable polymers. These blends form immiscible systems. Properties are ruled by composition of the blends and interaction between the constituents, which is reflected also in

Correspondence to: C. H. Chan (cchan@salam.uitm.edu.my).

Contract grant sponsor: Ministry of Science, Technology and Innovation (MOSTI), Malaysia; contract grant number: 03-01-01-SF0178.

thermal properties. Thermal properties influence development of morphologies that in turn strongly affect mechanical behavior. In blends where the crystalline constituent is in excess, this component crystallizes out from the melt, comprising a dispersion of ENR domains. At the opposite side of the composition scale, ENR being in excess, crystalline domains will develop in the ENR matrix. The main target here is to study the influence of ENR-dispersion and ENR-matrix on crystallization and melting of the crystalline constituents. As components combined with ENR, we selected poly(ethylene terephthalate) (PET), poly(3-hydroxybutyrate-*co*-3-hydroxyvalerate) with 12 mol % of hydroxyvalerate content (PHBV) and poly(ethylene oxide) (PEO). All of them exhibit appreciable crystallinity.

PET, a synthetic polyester, is an engineering polymer. PET is miscible with poly(ether imide)[20] and poly(vinylidene fluoride) (PVF_2)[21,22]; but is not miscible with poly(tetramethylene succinate),[23] ENR[24] and poly(ethylene napthalate-2,6-dicarboxylate) (PEN).[25] However, the compatibility of PET and PEN improves after transesterfication reaction.[25–30] PHBV is biodegradable aliphatic polyester. PHBV is miscible with PEO,[31] PVF_2[32] and poly(3-hydroxybutyrate)[33] but immiscible with poly(propylene carbonate),[34–36] poly(butylene succinate),[37] poly(ε-caprolactone) (PCL)[38] and ENR.[39] Lastly, PEO is synthetic biodegradable polyether. PEO is known to exhibit miscibility via hydrogen bonding or relatively weak dipole-dipole interactions with poly(vinyl alcohol),[40] poly(*p*-vinyl phenol),[41] cassava starch,[42] poly(*n*-butyl methacrylate)[43] and poly(L-lactide).[44] Properties have been reported on immiscible mixtures of PEO with PCL[45,46] and ENR with the addition of $LiClO_4$ as well.[3]

EXPERIMENTAL

Materials

Characteristics of polymers are listed in Table I. All the polymers were purified before further use. The chemical structures of the polymers are presented in Figure 1.

Preparation of the blends

Thin films of the ENR/PHBV and ENR/PEO blends were prepared by casting from 1% (w/w) solution of the two components in chloroform (Fisher Scientific, Leicestershire, UK) followed by evaporation of solvent at room temperature overnight and keeping afterwards the sample at 70°C under vacuum for 48 h. Blends of ENR and PET were prepared via precipitation method using phenol/1,2-dichloroethane (Fisher Scientific, Leicestershire, UK) in the ratio of 2:3 at the polymer concentration of 0.3 wt % as mutual solvent and methanol (Fisher Scientific, Leicestershire, UK) as the nonsolvent. The precipitates were filtered, followed by evaporation of the solvent under vacuum for 48 h at 50°C. Compositions of the blends ranged from 100/0 to 0/100 in steps of 10 wt %.

Thermal gravimetry analysis

Decomposition temperature (T_d) was determined by thermogravimetric analyzer (TGA) using Perkin–Elmer TGA 7 (Shelton, CT) under nitrogen gas purging. This analysis was used to study the thermal stability of the systems. The inflection points of the weight loss curves were taken as T_d. The samples were heated from 50 to 600°C at a rate of 20 K min^{-1}. Table I brings the results.

TABLE I
Characteristics of the Blends Constituents

Constituents	ENR with 50 mol% epoxy groups	PET	PHBV with 12 mol% HV	PEO
M_η[a]/kg mol^{-1}		18	–	300
M_w[b]/kg mol^{-1}	700	–	238	–
M_n[c]/kg mol^{-1}	200	–	109	–
T_d[d]/°C	412	447	269	440
T_m[e]/°C	–	235	161	66
T_c[f]/°C	–	214–228	105–112	44–54
T_g[g]/°C	−19	81	0	−54
ΔH_{ref}[h]/J g^{-1}	–	117.6	109	188.3
Supplier	Rubber Research Institute, Sungai Buloh, Malaysia	Sigma-Aldrich Chemical Co. (St. Louis, MO)		

[a] Viscosity-average molecular weight provided by the supplier.
[b] Weight-average of molecular weight as estimated in this work by Waters gel permeation chromatography (GPC). Polystyrene with low polydispersity was used as standard.
[c] Number-average molecular weight as estimated in this work by GPC.
[d] Decomposition temperature by thermogravimetry analysis as determined in this work.
[e] Melting temperature during first heating cycle as determined in this work.
[f] Range of isothermal crystallization temperature by DSC analysis
[g] Glass transition temperature after quench cooling as determined in this work.
[h] Melting enthalpy of 100% crystalline PET, [47] PHBV[48] and PEO.[49]

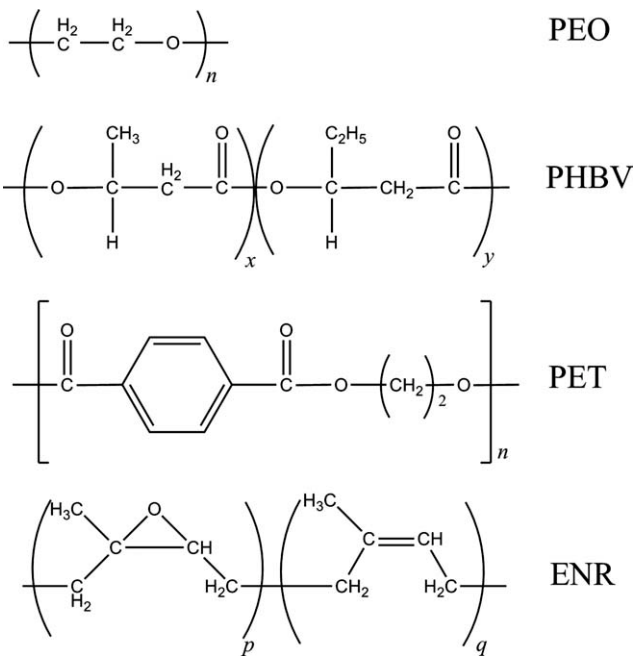

Figure 1 Chemical structures of polymers.

Differential scanning calorimetry

Perkin–Elmer DSC 7 (Shelton, CT) was used to study the crystallization and melting behavior and TA Q200 (Delware, USA) was used to study the glass transition temperature of the blends. Both of the DSCs were calibrated with indium and zinc standards and nitrogen atmosphere was purged throughout the analysis to minimize thermo-oxidative degradation. Samples with weight around 10 mg were used for each DSC experiment. The samples were exposed to different thermal histories:

Isothermal crystallization

Blends with PET, PHBV and PEO were annealed at annealing temperature T_a = 280, 175, and 80°C, respectively, for 1 min. Afterwards samples were cooled with a rate of 20 K min^{-1} to selected crystallization temperatures T_cs and crystallized for five half times of crystallization. Melting temperatures were determined in subsequent heating cycles with rates of 20 and 10 K min^{-1}, only for ENR/PHBV blends.

Glass transition temperature

The same procedure as in I except quenching of samples after annealing to temperatures well below −60°C and keeping there for 1 min.

Polarizing optical microscopy

Morphologies of blends were studied using Leica Q Win Software (Cambridge, UK) (for ENR/PET and ENR/PEO blends) or Image-Pro Express (for ENR/PHBV blends), which was attached to the Nikon microscope (Yokohama, Japan) equipped with a Linkam heating/cooling unit (Linkam TM 600/s) (Surrey, UK). Samples were subjected to the following thermal procedures:

Radial growth rate

Samples were exposed to heating and cooling cycles as in I. Micrographs were captured during isothermal crystallization in suitable time intervals and diameter of growing spherulites was determined.

Morphology for sample after isothermal crystallization

Heating and cooling cycles were applied as in Radial growth rate. Micrographs were taken after 60 min of crystallization at selected crystallization temperatures.

RESULTS AND DISCUSSION

Glass transition temperatures

The ENR blends were exposed to procedure II, described in Experimental section, to determine the glass transition temperature (T_g). Quantities T_g were taken from the second heating cycles at temperature, which characterizes half of the delta heat capacity of the DSC heat flow curve. The T_gs of the ENR blends, measured in the second heating cycle are depicted in Figure 2. Glass

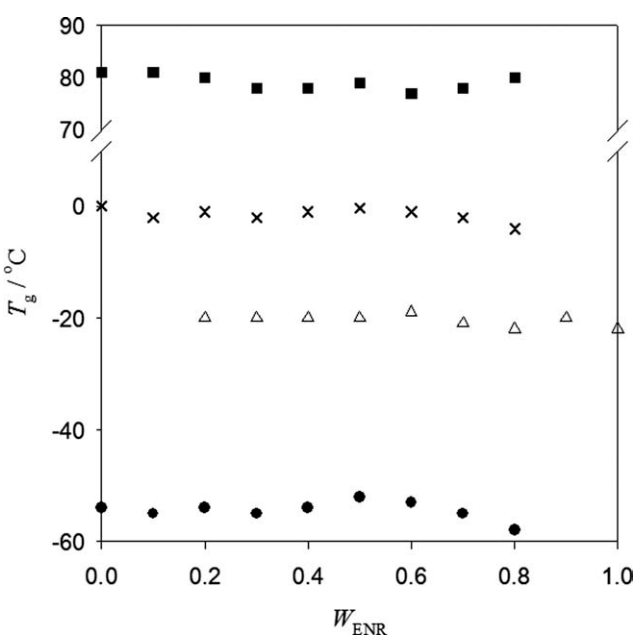

Figure 2 Glass transition temperatures, T_g, of ENR blends. ■, PET; ×, PHBV; Δ, ENR; ●, PEO.

transition temperatures of neat constituents are summarized in Table I. Two glass transition temperatures, corresponding to that of the neat constituents, were found for all blends and reflect immiscibility of the constituents.

Crystallinity in ENR blends

Melting enthalpies (ΔH_m) of crystallizable components were used to examine crystallinity (X^*) of the crystallizable component in the blends. Crystallinity is defined by the ratio $\Delta H_m/\Delta H_{\text{ref}}$ with ΔH_{ref} being the melting enthalpy of 100% crystalline polymer. The reference enthalpies for the polymers under discussion are listed in Table I. Quantity ΔH_m was determined according to thermal procedure I during reheating cycle after crystallization at selected crystallization temperatures for five half times. Half-time ($t_{0.5}$)is defined in the usual way as time taken for half of the crystallinity to develop during the isothermal crystallization process. This period of crystallization was selected to establish comparable levels of crystallinity in the blends.

PET and PEO in blends with ENR display only one melting peak in the DSC thermogram whereas double melting peaks occur in blends with PHBV after isothermal crystallization.[39] The double melting peaks are not well separated in most cases. Consequently, quantity ΔH_m refers to superposition of the melting peaks. Appreciable rates of crystallization could be observed for PEO, PHBV and PET at T_c = 49, 112, and 224°C, respectively. Undercoolings (ΔT_c) and corresponding crystallinities for the polymers are listed in Table II. Figure 3 reveals that crystallinity stays constant in the blends to a good approximation. The amorphous component does not influence crystallinity of the thermoplastics over a wide range of composition. Some scatter in crystallinity occurs only at high ENR content. This behavior does not change remarkably with crystallization temperature.

TABLE II
Crystallinities (X^*) and Undercoolings (ΔT_c) for the Semicrystalline Polymers

Polymer	T_c/°C	ΔT_c[a]/K	X^*/%
PET	224	46	39.5
PHBV	112	83	50.3
PEO	49	29	54.2

[a] Undercooling, $\Delta T_c \equiv T_m^o - T_c$, T_m^o – equilibrium melting temperature.

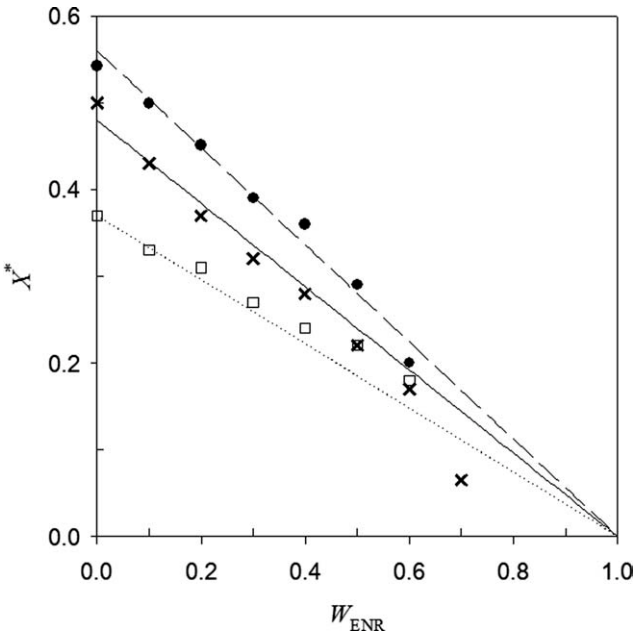

Figure 3 Crystallinity in ENR blends as a function of weight fraction of ENR; curves represent constant crystallinity in the blends. □, PET crystallized at T_c = 224°C; ×, PHBV at T_c = 112°C and ●, PEO at T_c = 49°C.

Melting behavior in ENR blends

Melting temperatures (T_m) were measured in the reheating cycle after samples were crystallized isothermally for five half times ($t_{0.5}$) at the respective crystallization temperature according to thermal procedure I. The equilibrium melting temperature (T_m^o) was determined after Hoffman-Weeks method adopting a linear relationship between crystallization and melting temperature[50]

$$T_m = \gamma T_c + (1 - \gamma) T_m^o \quad (1)$$

where parameter γ = const represents the change of melting temperature with crystallization temperature, dT_m/dT_c.

As mentioned before PET and PEO display only one melting endotherm in the DSC thermogram whereas PHBV exhibits two. For the former constituents, the maximum peak of the melting endotherm was taken as apparent melting temperature. The lower melting endotherm was used for determination of apparent melting temperature of PHBV since only this peak shifts with crystallization temperature.

Hoffman-Weeks plots for PHBV and PEO are shown in Figure 4. Analogous results were obtained for PET. Also for the blends, we found linear variation of melting temperature with crystallization temperature. The slopes γ fall in the range of 0.30–0.46. Results, listed in Table III, shows constancy of equilibrium melting points over wide ranges of respective blend compositions.

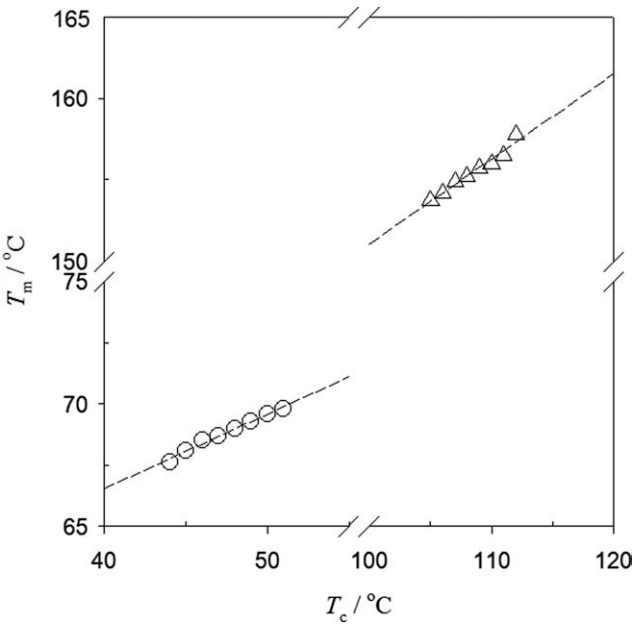

Figure 4 Hoffman-Weeks plots for semicrystalline polymers; Δ, PHBV and ○, PEO.

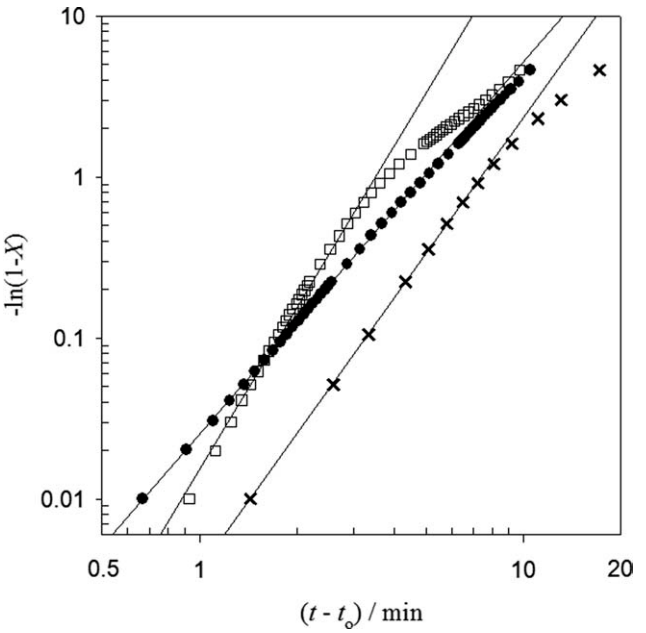

Figure 5 Avrami plots of neat semicrystalline polymers. □, PET at crystallization temperature T_c = 224°C, ×, PHBV at T_c = 112°C, and ●, PEO at T_c = 49°C. The solid curves represent linear regression curves after eq. (2).

Kinetics of isothermal crystallization of crystallizable component in ENR blends

Isothermal crystallization experiments were carried out according to thermal procedure I, as described in the Experimental part. The overall crystallization rate can be monitored by thermal analysis through the evolution of heat of crystallization by DSC. In the heterogeneous system under discussion, phase boundaries or morphology of the ENR blends might also influence the overall rate of crystallization of the crystallizable component. Therefore, application of Avrami equation[51] is restricted to the neat semicrystalline polymers.

$$X(t) = 1 - \exp[-K^{1/n}t]^n \quad (2)$$

The degree of conversion $X(t)$ is the normalized crystallinity given as the ratio of the degree of crystallinity at time t and the final degree of crystallinity.

TABLE III
Equilibrium Melting Temperature and Parameter γ for Crystallizable Components in ENR Blends After Hoffman-Weeks

	T_m°/°C (γ)		
W_{ENR}	PET	PHBV	PEO
0	270 (0.37)	195 (0.46)	78 (0.31)
0.3	271 (0.37)	194 (0.39)	79 (0.29)
0.5	271 (0.36)	194 (0.42)	77 (0.37)
0.6	270 (0.33)	188 (0.46)	74 (0.30)
0.7	–	194 (0.46)	–

Rate constant of isothermal crystallization ($K^{1/n}$) and Avrami exponent (n) can be extracted from intercept and slope of a double-logarithmic plot after eq. (2). Parameter $K^{1/n}$ represents the overall kinetic rate constant and n is a parameter, which depends on the type of nucleation and the geometry of growing crystals. The confidence intervals of overall rate constant and Avrami exponent refer solely to the regression analysis using two-tailed student t-test with 95% of confidence level for only one experiment.

Avrami plots for neat PET, PHBV, and PEO are strictly linear up to conversions of 60% (correlation coefficients >0.995) as depicted in Figure 5. Table IV shows Avrami coefficients for neat semicrystalline polymers at preselected undercoolings as stated in Table II. We note that the Avrami exponents for PET > PHBV > PEO are 3.5, 3, and 2.2, respectively. Table IV lists also the half times calculated after eq. (2) with the Avrami parameters.

The rate of crystallization of crystallizable component in ENR blends is characterized by the experimentally determined reciprocal half-time, $(t_{0.5})^{-1}$. In this study, half times of isothermal crystallization were estimated from the area of the exotherm at T_c = const. In addition, results for neat crystallizable component may serve as reference for evaluation of crystallization of the crystallizable component in ENR blends. We note that the experimentally determined $(t_{0.5})^{-1}$ for the crystallizable component in the blends as shown in Figure 6 is consistent with the quantities of $(t_{0.5})^{-1}$ estimated from eq. (2). In all cases, the error of these quantities is less than 5%.

TABLE IV
Rate of Crystallization ($K^{1/n}$) and Avrami Exponent (n) for the Semicrystalline Polymers

Polymer	T_c/°C	ΔT_c/K	$K^{1/n}$/min^{-1}	n	r^a	$(t_{0.5})^{-1}$ / min^{-1}
PET	224	46	0.286 ± 0.004	3.39 ± 0.10	0.995	0.32
PHBV	112	83	0.17 ± 0.02	2.96 ± 0.08	0.9996	0.19
PEO	49	29	0.197 ± 0.002	2.23 ± 0.02	0.9994	0.23

[a] Correlation coefficient.

We recognize an exponential decay of the rate with increasing $(\Delta T_c)^{-1}$ that is with approach to equilibrium melting temperature. Experimental data obey the following relationship to a good approximation.

$$(t_{0.5})^{-1} = A \exp\left(-\frac{B}{\Delta T_c}\right) \quad (3)$$

Quantity B might be related to the ratio of energy densities in lamella fold surface and bulk formulated with use of Kelvin equation as follows

$$B \equiv \frac{2T_m^o}{\gamma} \frac{(\sigma/l_c)}{\rho \Delta H_{spec}} \quad (4)$$

where (σ/l_c) marks surface energy density of a lamella grown at crystallization temperature T_c. The ratio of energy densities can be also related to the ratio of entropies giving the distance to equilibrium

$$-\frac{1}{\Delta s}\left(\frac{\partial s_a}{\partial X}\right)_o = \frac{2(\sigma/l_c)}{\rho \Delta H_{spec}} \quad (5)$$

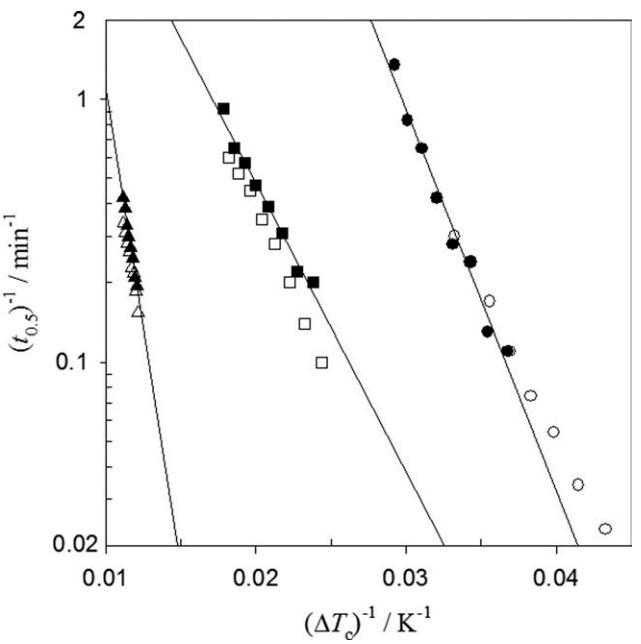

Figure 6 Rate of isothermal crystallization versus reciprocal undercooling. ■, PET; ▲, PHBV, and ●, PEO. Open markers corresponds to the respective 50/50 ENR blends.

The derivative on the left-hand side represents the change of entropy in the amorphous phase with degree of crystallinity and Δs is the entropy change at equilibrium. With eq. (3), we recognize that the ratio of energy densities acts as driving force for crystallization. Results are listed in Table V. For PHBV, we need a high undercooling to get an appreciable rate of crystallization. Only when the polymer is far away from equilibrium, the necessary driving force for crystallization exists and it crystallizes with a sufficiently high rate. The lowest undercooling for an acceptable rate of crystallization, we need for PEO. To compare the rates at ΔT_c = const, one sees that at $(\Delta T_c)^{-1} = 0.03$ K^{-1}, the rate for PEO is $(t_{0.5})^{-1} = 1$ min^{-1}; however, for PHBV almost eight orders of magnitude lower. Table V also shows that only minor changes of rate of crystallization might be observed in blends with ENR. This is nicely confirmed by the growth rates of spherulites shown in Figure 7.

Blend morphologies

Before presenting the morphologies, we note that, we selected undercoolings in a way that rate of crystallization was roughly equal for all blends. This can be easily verified from Figure 6 with the undercoolings given in Table II. Figure 8 shows a symmetric blend of ENR and PET. Small spherulites indicate a high density of growing nuclei. Moreover, development of small spherulites is in accordance with the low value of the ratio of surface to bulk energy for PET as given in Table V. We recognize formation of cocontinuous morphology. Phase inversion to PET dispersion in the ENR matrix fully develops in 70/30 blend of ENR with PET. One also observes ENR inclusions in PET domains. This is due to higher elasticity of the ENR component as compared to PET.

TABLE V
Parameter B and Ratio of Energy Densities after eqs. (3) and (4)

	$W_{ENR} = 0$		$W_{ENR} = 0.5$	
ENR blends	B/K	$\frac{(\sigma/l_c)}{(\rho \Delta H_{spec})}$	B/K	$\frac{(\sigma/l_c)}{(\rho \Delta H_{spec})}$
PEO	334	0.15	262	0.14
PHBV	833	0.41	816	0.37
PET	253	0.086	295	0.090

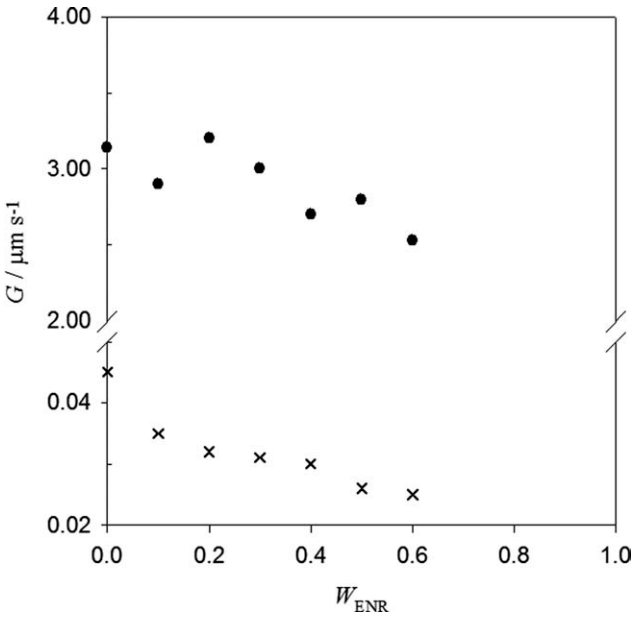

Figure 7 Radial growth rates of spherulites as a function of mass fraction of ENR. ×, PHBV at $T_c = 120°C$, and ●, PEO at $T_c = 49°C$.

Figure 9 presents the morphology of a 50/50 blend of ENR with PHBV. We recognize a remarkable difference to blends with PET. PET develops the lowest ratio of energy densities in surface and bulk of crystallite whereas PHBV generates the highest value (cf. Table V). Moreover, Table I tells us that PET and PHBV have approximately the same bulk energies. As a consequence, values of the energy ratio indicate for PHBV a much higher interfacial tension of the crystallite to the amorphous surrounding than for PET, around five times higher. The relatively high surface tension leads to formation of large spherulites. As a result, also large domains of ENR are included in the crystalline regions.

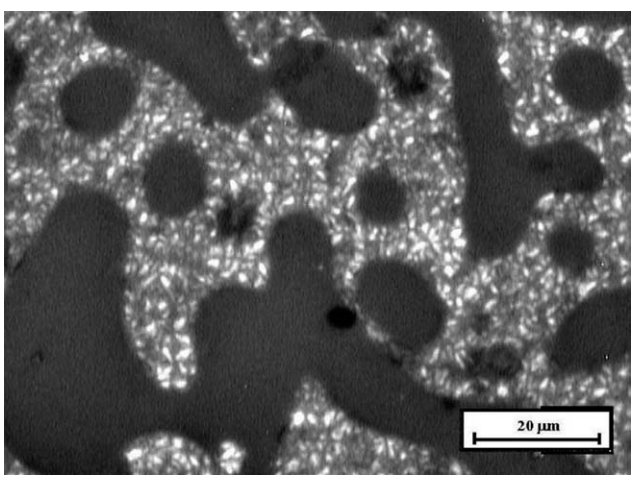

Figure 8 Morphology of a symmetric ENR/PET blend; the micrograph was taken at 224°C after crystallizing the sample for 60 min; magnification: ×50.

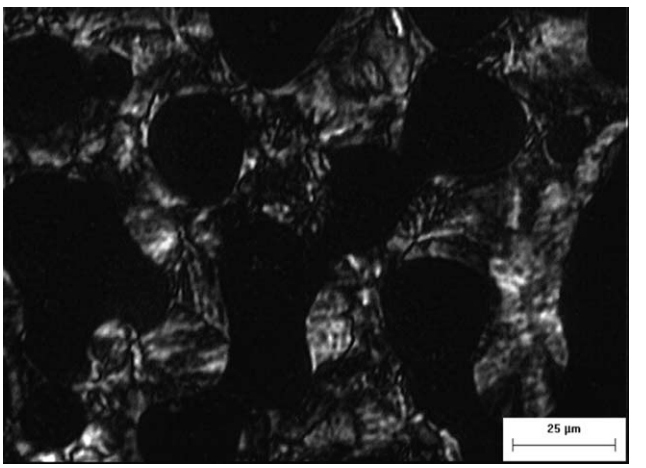

Figure 9 Morphology in a symmetric ENR/PHBV blend; the micrograph was taken at 112°C after crystallizing the sample for 60 min; magnification: ×40.

Morphology in a 50/50 blend of ENR and PEO is shown in Figure 10. Data after Hoffman-Weeks, presented in Table III, reveal that crystallization of PEO proceeds much closer to equilibrium as that of the other polymers. Therefore, large spherulites develop. However, the ratio of energy densities of Table V indicates a low interfacial free energy of PEO as compared to PHBV, since we have to take into account that the bulk energy of PEO is almost twice that of PHBV. Owing to the low interfacial energy of PEO crystallites, ENR inclusions cause irregular deformation of spherulites. Stability of supermolecular structures in blends with PEO is low. These structures are prone to decay in smaller crystalline regions. At sufficiently high content of ENR, spherulites cannot be formed anymore.

In summary, thermal and morphological studies show that the aromatic polyester develops the weakest adhesion to ENR whereas the aliphatic generates

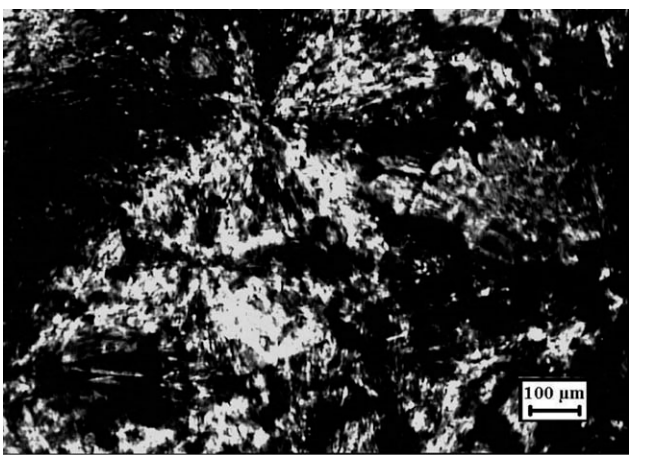

Figure 10 Morphology in a symmetric ENR/PEO blend; the micrograph was taken at 49°C after crystallizing the sample for 60 min; magnification: ×5.

the strongest. However, supermolecular structures remain stable, only in blends with PEO they tend to decay.

CONCLUSIONS

The study presents thermal properties and morphologies of ENR-based blends with three thermoplastics, PET, PHBV, and PEO. Glass transition temperatures reveal that these blends are completely immiscible in the molten state. Degrees of crystallinity are not influenced by the amorphous component. Morphology development in the blends was studied at different deviations from equilibrium, but under condition of constant rate of crystallization. Rates of crystallization descend exponentially with undercooling. Corresponding driving forces for crystallization might be related to the ratio of energy densities in surface and bulk of the crystallites. This allows for correlation of morphologies to the ratio of energy densities. It turns out that only weak adhesion exists between PET and ENR whereas PHBV establishes much stronger affinity to ENR. Supermolecular structures of PEO are unstable in blends with ENR owing to low interfacial energy of crystallite to amorphous surrounding. Stability of these structures is not influenced in ENR-blends with PET and PHBV.

Special thanks are dedicated to Nawiwi M. A. who provided results that were incorporated in this study.

References

1. Asaletha, R.; Kumaran M. G.; Thomas, S. Eur Polym Mater 1999, 35, 253.
2. Jansen, P.; Gomes, A. S.; Soares, B. G. J Appl Polym Sci 1996, 61, 591.
3. Chan, C. H.; Kammer, H. W. J Appl Polym Sci 2008, 110, 424.
4. Ray Chowdhury, S.; Mishra, J. K.; Das, C. K. Polym Degrad Stab 2000, 70, 199.
5. Chan, C. H.; Ismail, J.; Kammer, H. W. Polym Degrad Stab 2004, 85, 947.
6. Shibanov, Y. D.; Godovski, Y. K. Progr Colloid Polym Sci 1989, 80, 110.
7. Oudhuis, A. A. C. M.; Thieves, H. J.; van Hutten, P. F.; ten Brinke, G. Polymer 1994, 35, 3937.
8. Kammer, H. W.; Kummerlöwe, C. In Adv in Polymer Blends and Alloys Technology; Finlayson, K.; Ed.; Vol. 5, Technomic Publ: Lancaster, Penns, 1994; p 132.
9. Dreezen, G.; Zang, F.; Groenincks, G. Polymer 1999, 40, 5907.
10. Groeninckx, G.; Vanneste, M.; Everaert, V. In Polymer Blends Handbook, Vol1; Utracki, L. A., Ed.; Kluwer Academic Publishers: Dordrecht, Boston, London 2002; p 203.
11. Gelling, I. R. Rubber Chem Technol 1985, 58, 86.
12. Baker, C. S. L.; Gelling, I. R.; Newell, R. Rubber Chem Technol 1985, 58, 67.
13. Kallitsis, J. K.; Kalfoglou, N. K. J Appl Polym Sci 1989, 37, 453.
14. Mohamad, Z.; Ismail, H.; Chantara Thevy, R. J Appl Polym Sci 2006, 99, 1504.
15. Varughese, K. T.; Nando, G. B.; De, P. P.; De, S. K. J Mater Sci 1988, 23, 3894.
16. Varughese, K. T.; Nando, G. B.; De, P. P. J Mater Sci 1988, 23, 3903.
17. Mohanty, S.; Nando, G. B.; Vijayan, K.; Neelakanthan, N. R. Polym 1996, 37, 5387.
18. Mohanty, S.; Roy, S.; Santra, R.; Nando, G. B. J Appl Polym Sci 1985, 58, 1947.
19. Lee, H. K.; Ismail, J.; Kammer, H. W.; Bakar, M. A. J Appl Polym Sci 2005, 95, 113.
20. Chen, H. L.; Hsiao, M. S. Macromol 1998, 31, 6579.
21. Habibur Rahman, M.; Nandi, A. K. Polym 2002, 43, 6863.
22. Rahman, M. H.; Nandi, A. K. Macromol Chem Phys 2002, 203, 653.
23. Chong, K. F.; Schmidt, H.; Kummerlöwe, C.; Kammer, H. W. J Appl Polym Sci 2004, 92, 149.
24. Sulaiman, S. F.; Chan, C. H.; Harun, M. K. Mater Res Innov 2009, 13, 225.
25. Wagner, M. H.; Wu, W.; Liu, Y.; Qian, Q.; Zhang, Y.; Mielke, W. J Appl Polym Sci 2008, 110, 177.
26. Patcheak, T. D.; Jabarin, S. A. Polym 2001, 42, 8975.
27. Collins, S.; Kenwright, A. M.; Pawson, C.; Peace, S. K.; Richards, R. W. Macromol 2000, 33, 2974.
28. Bravard, S. P.; Boyd, R. H. Macromol 2003, 36, 741.
29. Aoki, Y.; Li, L.; Amari, T.; Nishimura Arashiro, K. Y. Macromol 1923 1999, 32.
30. Andresen, E.; Zachmann, H. G. Colloid Polym Sci 1994, 272, 1352.
31. Tan, S. M.; Ismail, J.; Kummerlöwe, C.; Kammer, H. W. J Appl Polym Sci 2006, 101, 2776.
32. Qiu, Z. B.; Fujinami, S.; Komura, M.; Nakajima, K.; Ikehara, T.; Nishi, T. Polym 2004, 45, 4355.
33. Chan, C. H.; Kummerlöwe, C.; Kammer, H. W. Macromol Chem Phys 2004, 205, 664.
34. Tao, J; Song, C.; Cao, M.; Hu, D.; Liu, L.; Liu, N.; Wang, S. Polym Degrad Stab 2009, 94, 575.
35. Li, J.; Lai, M. F.; Liu, J. J. J Appl Polym Sci 2004, 92, 2514.
36. Li, J.; Lai, M. F.; Liu, J. J. J Appl Polym Sci 2005, 98, 1427.
37. Qui, Z. B.; Ikehara, T.; Nishi, T. Polym 2003, 44, 7519.
38. Qiu, Z. B.; Yang, W.; Ikehara, T.; Nishi, T. Polym 2005, 46, 11814.
39. Chan, C. H.; Kammer, H. W. Polym Bull 2009, 63, 673.
40. Sotele, J. J.; Soldi, V.; Pires, A. T. N. Polym 1997, 38, 1179.
41. Pedrosa, P.; Pomposo, J. A.; Calahorra, E.; Cortazar, M. Polym 1995, 36, 3889.
42. Pereira, A. G. B.; Gouveia, R. F.; de Carvalho, G. M.; Rubira, A. F.; Muniz, E. C. Mater Sci Eng C 2009, 29, 499.
43. Shafee, E.; El.; Ueda, W. Eur Polym Mater 2002, 38, 1327.
44. Nijenhuis, A. J; Colstee, E.; Grijpma, D. W. Polym 1996, 37, 5849.
45. Qiu, Z.; Ikehara, T.; Nishi, T. Polym 2003, 44, 3101.
46. Chee, M. J. K.; Ismail, J.; Kummerlöwe, C.; Kammer, H. W. Polymer 2002, 43, 1235.
47. Groeninckx, G.; Reynaers, H.; Berghmans, H.; Smets, G. J Polym Sci, Polym Phys Ed 1980, 18, 1311.
48. Scandola, M.; Focarete, M. L.; Adamus, G.; Sikorska, W.; Baranowska, I.; Swierczek, S.; Gnatowaski, M.; Kowalczuk, M.; Jedlinski, Z. Macromol 1997, 30, 2568.
49. Cimmino, S.; Di Pace, E.; Martuscelli, E.; Silvestre, C. Makromol Chem 1990, 191, 2447.
50. Hoffman, J. D.; Weeks, J. J. J Res Natl Bur Stand (A) 1962, 66, 13.
51. Avrami, M. J Chem Phys 1939, 7, 1103.